Nucleic Acids Research, 2006, Vol. 34, No. 7 ***e53***
doi:10.1093/nar/gkl143

Polycistronic RNA polymerase II expression vectors for RNA interference based on BIC/miR-155

Kwan-Ho Chung[1,2], Christopher C. Hart[1,2], Sarmad Al-Bassam[1], Adam Avery[3], Jennifer Taylor[3], Paresh D. Patel[1,2,4], Anne B. Vojtek[3] and David L. Turner[1,2,3,*]

[1]Molecular and Behavioral Neuroscience Institute, [2]Program in Neuroscience, [3]Department of Biological Chemistry and [4]Department of Psychiatry, University of Michigan, Ann Arbor, MI 48109-2200, USA

Received February 14, 2006; Revised March 9, 2006; Accepted March 16, 2006

ABSTRACT

Vector-based RNA interference (RNAi) has emerged as a valuable tool for analysis of gene function. We have developed new RNA polymerase II expression vectors for RNAi, designated SIBR vectors, based upon the non-coding RNA BIC. BIC contains the miR-155 microRNA (miRNA) precursor, and we find that expression of a short region of the third exon of mouse BIC is sufficient to produce miR-155 in mammalian cells. The SIBR vectors use a modified miR-155 precursor stem–loop and flanking BIC sequences to express synthetic miRNAs complementary to target RNAs. Like RNA polymerase III driven short hairpin RNA vectors, the SIBR vectors efficiently reduce target mRNA and protein expression. The synthetic miRNAs can be expressed from an intron, allowing coexpression of a marker or other protein with the miRNAs. In addition, intronic expression of a synthetic miRNA from a two intron vector enhances RNAi. A SIBR vector can express two different miRNAs from a single transcript for effective inhibition of two different target mRNAs. Furthermore, at least eight tandem copies of a synthetic miRNA can be expressed in a polycistronic transcript to increase the inhibition of a target RNA. The SIBR vectors are flexible tools for a variety of RNAi applications.

INTRODUCTION

RNA interference (RNAi) has become a commonly used tool for the analysis of gene function in animals and plants [for reviews see (1–3)]. Short-interfering RNAs (siRNAs) of about 21–23 nt can be produced within a cell by Dicer processing of double-stranded RNAs or hairpin RNAs. Alternately, synthetic siRNA duplexes can be introduced into cells by transfection. In both cases, siRNAs enter the RNA-induced silencing complex (RISC) and guide cleavage and degradation of endogenous mRNAs that contain sequences perfectly or near-perfectly complementary to the siRNAs. siRNA-mediated recognition of target mRNAs is highly sequence specific. Animal cells contain numerous endogenous ~22 nt RNAs known as microRNAs (miRNAs) (4–6) that also can guide cleavage of RNAs with near-perfect complementary matching sequences (7–9). In addition, miRNAs also can cause mRNA degradation and/or translational inhibition when bound to partially complementary sites in the 3′-untranslated region (3′-UTR) of mRNAs (10–14).

Cellular miRNAs are derived by processing from 60 to 70 nt stem–loop precursors [reviewed in (15)]. However, miRNA precursors are initially synthesized as part of longer primary RNA transcripts (pri-miRNAs) (16). Most pri-miRNAs appear to be synthesized by RNA polymerase II (17,18). The nuclear endonuclease Drosha cleaves a pri-miRNA to release the stem–loop miRNA precursor (pre-miRNAs) (19). The stem–loop miRNA precursor is exported from the nucleus and subsequently processed by Dicer to release the mature miRNA in the cytoplasm. While Dicer processing produces a short RNA from each arm/strand of the stem–loop precursor, only one of these two potential miRNAs stably accumulates in most cases. A number of miRNAs are present in genomic clusters that appear to be transcribed as polycistronic pri-miRNAs, allowing the production of multiple miRNAs from a single transcription unit (16,20,21). Some miRNA precursors are located in the introns of protein coding genes and can be coexpressed with the mature mRNAs from the same genes, suggesting that miRNA precursors can be excised from introns without disrupting production of the mRNA (22) (M. Deo, J.-Y. Yu, K.-H. Chung, M. Tippens, and D. L. Turner, manuscript submitted).

We and others have developed DNA expression vectors for RNAi in mammalian cells that express short hairpin RNAs (shRNAs) under the control of a RNA polymerase III promoter

*To whom correspondence should be addressed. Tel: +734 647 6891; Fax: +734 936 2690; Email: dlturner@umich.edu

[for reviews see (2,23,24)]. shRNAs resemble the short stem–loop structure of endogenous miRNA precursors, allowing the shRNAs to enter the miRNA synthetic pathway and be processed by the Dicer endonuclease into ~21 nt siRNAs/miRNAs. Although shRNA vectors are widely used as tools for the analysis of gene function, existing shRNA vectors have some limitations. Only a single shRNA is expressed from each RNA polymerase III promoter, so the inhibition of multiple genes requires multiple promoters or vectors (25,26). This causes a concern that the shRNAs may not always be coexpressed at similar levels, even when present on the same plasmid. Also, identification of cells expressing an introduced shRNA usually requires coexpression of a marker protein from a separate RNA polymerase II promoter. In this situation, the marker may not always be coregulated with the shRNA. In addition, regulated expression from RNA polymerase III promoters is often more difficult in comparison with RNA polymerase II driven promoters. RNAi expression vectors that use RNA polymerase II could potentially overcome many of these limitations. Cullen and colleagues described a vector for RNAi in which a synthetic siRNA/miRNA is expressed from a synthetic stem–loop precursor based on the miR-30 miRNA precursor (27,28). Subsequently, other groups have developed additional miR-30 based vectors for RNAi (29–32). Davidson and colleagues also described an RNAi vector in which a synthetic stem–loop was expressed from a capped and polyadenylated RNA pol II transcript (33). Recently, a transgenic mouse for tissue-specific RNAi has been generated by introducing an shRNA into the intron of artificial non-coding RNA polymerase II RNA (34).

BIC is an evolutionarily conserved non-coding RNA that cooperates with c-myc to cause lymphoma in chickens when either inappropriately activated by insertion of a retrovirus or ectopically expressed in a retroviral vector (35–37). The stem–loop precursor for the mouse miR-155 miRNA is located within the third exon of the mouse BIC gene (38). The minimal described oncogenic domain for chicken BIC contains the miR-155 precursor and some flanking sequences, suggesting that main function of BIC may be to produce miR-155. The ability to express functional BIC (and presumably miR-155) from a heterologous RNA polymerase II promoter in a retroviral vector (39) suggested that BIC/miR-155 might be a good sequence framework for construction of RNA polymerase II-based RNAi vectors. Here we describe a novel vector system for mammalian RNAi based upon BIC and the miR-155 miRNA precursor. These vectors use standard RNA polymerase II promoters to express a synthetic miRNA (siRNA) directed against a target mRNA and provide effective inhibition in mammalian cells. At least two different synthetic miRNAs can be expressed from a single transcript without compromising their processing or inhibitory efficacy, allowing effective inhibition of two genes using a single vector. Alternately, multiple tandem copies of a miRNA can be expressed in a single polycistronic transcript for increased inhibition. In addition, the sequences necessary for producing the synthetic miRNAs can be located within an intron, allowing coupled expression of the miRNA and a marker protein from the same transcript. Interestingly, expression of a synthetic miRNA from a two intron vector further enhanced RNAi. The miR-155 based vector system offers a flexible system for the expression of multiple miRNAs combined with protein marker expression using a single polycistronic transcription unit.

MATERIALS AND METHODS

Cell culture and transfection

Mouse P19 cells were cultured as described (40). For luciferase assays, $\sim 7 \times 10^4$ cells were plated per one well on a 12-well plate and transfected 24 h later. Transfections were performed with Lipofectamine 2000 (Invitrogen) as directed by the manufacturer. The transfection efficiency for P19 cells was ~50%. For northern blotting, $\sim 1 \times 10^5$ cells were plated in a 35 mm dish and transfected 24 h later using FuGene6 (Roche).

Plasmids

Plasmids were constructed using standard molecular biology techniques. Part of the third BIC exon (99–554 nt, based on accession AY096003) was amplified by PCR from mouse genomic DNA and inserted into the CS2+ vector (41,42). Deletions were constructed using PCR with appropriate primers. To construct the SIBR cassette, the miR-155 precursor stem–loop in BIC 134–283 was replaced with a synthetic polylinker containing two inverted Bbs1 (New England Biolabs) sites. SIBR cassettes targeting various mRNAs were constructed by ligation of 64 nt DNA oligonucleotide duplexes to Bbs1 cut SIBR vectors (see Figure 2A and Table 1 for sequences). Constructs were verified by DNA sequencing. US2 was constructed by replacing the simian CMV promoter in CS2+ with the human ubiquitin C (ubC) promoter, first ubC exon (non-coding), and first ubC intron from pUB GFP (43) (gift of T. Matsuda and C. Cepko). US2-Ngn2 contains the mouse neurogenin2 coding region isolated by PCR (J.-Y. Yu and D.L. Turner, unpublished data). US2-MT expresses six multimerized myc-epitope tags, while US2-GFP expresses enhanced green fluorescent protein (GFP) (Clontech). UI2 is a derivative of US2 that has the SIBR cassette inserted into a non-conserved region in the ubC intron in US2, as well as a number of restriction site changes to facilitate construction of derivatives. GFP or the puromycin resistance protein is present in the second exon of UI2-GFP-SIBR and UI2-puro-SIBR respectively. The UI4-GFP-SIBR vector contains the ubC promoter, the first non-coding ubC exon, and first ubC intron, followed by a short non-coding second exon (derived from ubC exon 2 and rabbit globin exon 2 sequences), followed by the second intron from the rabbit globin gene. The third exon of UI4-GFP-SIBR contains the GFP coding region, while the SIBR cassette is inserted into the middle of the second intron, along with flanking restriction sites to facilitate construction of tandem SIBR cassettes (sites are identical to UI2). The remainder of the vector is identical to UI2-GFP-SIBR. Vectors with tandem luc-1601 or B-Raf + c-Raf SIBR cassettes were constructed by excising a SalI-XbaI flanked SIBR cassette and inserting it between the XhoI and XbaI sites in the same vector (see Figure 8A and B for schematic). The same procedure using the UI2-GFP-SIBR Luc-1601×2 vector was used to construct the UI2-GFP-SIBR Luc-1601×4 vector and was repeated with the UI2-GFP-SIBR Luc-1601×4 vector to construct UI2-GFP-SIBR Luc-1601×8.

Table 1. Sequences and predicted precursor structures for miR-155 and synthetic miRNAs used in the SIBR vectors

Mouse miR-155 (AY096003)	…UUAAUGCUAAUUGUGAUAGGGGuuuuggcc …acAAUUACGAUUG-UCC-AUCCUCagucaguc
Human miR-155 (AF402776)	…UUAAUGCUAAUCGUGAUAGGGGuu-uuugc …acAAUUACGAUUA-UAC-AUCCUCagucaaccu
Chicken miR-155 (AF182318)	…UUAAUGCUAAUCGUGAUAGGGGuu-uuuac …acAAUUACGAUU-GUAC-AUCCUCaguaagucu
Luc-1601 (U47298)	…UUUAUGAGGAUCUCUCUGAUUUuuuuggcc …acAAAUACUCCU-GAGA-ACUAAAagucaguc
GAPDH-240 (NM_001001303)	…UUGAUGACAAGCUUCCCAUUCUuuuuggcc …acAACUACUGUUU-AAGG-UAAGAagucaguc
GAPDH-528	…UCAUGGAUGACCUUGGCCAGGGuuuuggcc …acAGUACCUACUGAA--CGGUCCCagucaguc
HP1γ-664 (AK083957)	…UAAUUCAAAACCCAAGAUCCAGuuuuggcc …acAUUAAGUUUUGGA--UUAGGUCagucaguc
HP1γ-903	…UAACUGUAAAAUCUCCCCAGCGuuuuggcc …acAUUGACAUUUUGU--GGGUCGCagucaguc
Rassf1-1346 (BC002173)	…UAAGAGGGAACCCCAGACUCUAuuuuggcc …acAUUCUCCCUUGGC--UUGAGAUagucaguc
Rassf1-1623	…UAUUCAGCCAAUUCUCUCAGGCuuuuggcc …acAUAAGUCGGUUG-GA-AGUCUGagucaguc
B-Raf-2023 (M64429)	…UUACUUUAAUGUCUCACUCAGGuuuuggcc …acAAUGAAAUUAU-G-GCGAGUUCagucaguc
c-Raf-2268 (AB057663)	…UAUGAAGUUAAGGCCCUGUGAGuuuuggcc …acAUACUUCAAUUU--GGACACUCagucaguc
Posh-2852 (AF030131)	…UAAGCUUUCUCCGUGUCCCGUCuuuuggcc …acAUUCGAAAGAG-UAC-GGGCAGagucaguc
ND1-380 (AK005073)	…UAAUUUAAAACGUUCUAGGCGCuuuuggcc …acAUUAAAUUUUG-GAG-UCCGUGagucaguc
Tubb3-1512 (AF312873)	…UUAACCUGGGAGCCCUAAUGAGuuuuggcc …acAAUUGGACCCU-GA-GUUACUCagucaguc
Tubb3-1549	…ACAGAGCCAAGUGGACUCACAUuuuuggcc …acUGUCUCGGUUC-UCU-AGUGUAagucaguc

The expected mature miRNA (underlined) and its complement are in upper case, while the loop and two base 3′ overhang (shared by all precursors) are shown in lower case. Watson–Crick basepairs are indicated by lines; GU basepairs indicated by two dots. The mfold program was used to predict precursor structures (62). Accession numbers for the BIC RNAs and for each target mRNA are given (synthetic miRNAs are named by the position of the first matching base of the target mRNA).

The UAS-luc reporter and tamoxifen-inducible CS2+G4D-ER™-G4A activator vector have been described previously (25). For the UAS-luc-miR-155as reporter, a sequence complementary to miR-155 was introduced by PCR into the UAS-luc vector after the stop codon of luciferase gene. The UAS-luc-Tubb3-UTR reporter was also constructed in the same way by using PCR primers spanning most of the 3′-UTR of Tubb3 (1387–1684 nt from NM023279). The UAS-luc-ND1-UTR reporter contains the entire mouse NeuroD1 3′-UTR (1161–2495 nt from AK005073) (44) inserted into UAS-luc after the luciferase coding region.

Additional vector information and sequences are available at http://sitemaker.umich.edu/dlturner.vectors.

Luciferase reporter assays

Luciferase assays were done essentially as described, using an inducible luciferase target (25), except that the medium was changed to fresh MEMα medium with 1 μM 4-OH-tamoxifen (Sigma) 24 h after transfection, and cells were lysed 45–48 h after transfection. The DNA amounts per one well of a 12-well plate were as follows: UAS-luc, UAS-luc-miR-155as, UAS-luc-ND1-3′-UTR or UAS-luc-Tubb3-3′-UTR, 80 ng; CS2+cβgal, 50 ng; CS2+G4D-ER™-G4A, 100 ng; CS2+SIBR, US2-SIBR, UI2-SIBR or UI4-SIBR expression vectors, 400 ng. For the experiments in Figures 7 and 9, the expression vectors were 100, 200 or 400 ng, with US2-MT added to maintain a constant DNA amount per well (other plasmid amounts as above). Reporter activity was assayed by using the Dual-Light system (Applied Biosystems) and was normalized to β-galactosidase activity to control for transfection efficiency variation among different wells. All reporter assays shown are based on data averaged from at least three independent transfections.

Northern blotting

P19 cells were transfected with 4 μg of CS2 + SIBR expression vectors per 35 m dish and lysed at ∼24 h after transfection for total RNA isolation using TRIzol (Invitrogen). RNA was (15 μg) separated by elecrophoresis on 18% polyacrylamide denaturing gels, transferred with a GENIE electroblotter (Idea Scientific) onto Hybond-N+ membrane (Amersham Pharmacia Biotech), and ultraviolet crosslinked. DNA oligonucleotide probes and RNA oligonucleotide size markers were 5′ end labeled with [α-^{32}P]ATP using T4 polynucleotide kinase. Hybridization was performed at 42°C in Church–Gilbert solution (1 mM EDTA, 0.25 M Na_2HPO_4, 7% SDS) overnight. Membranes were washed at 42°C, twice with 2× SSPE/0.1% SDS and once with 0.5× SSPE/0.1% SDS. Blots were exposed in the Storage Phosphor Screen (Molecular Dynamics) at room temperature for 48–72 h. Images were obtained with IPLab Gel H 1.5 g software (Signal Analytics) from PhosphorImager 445 SI (Molecular Dynamics). Blots were stripped by boiling in 0.1% SDS/0.1× SSC solution for 20 min for reprobing.

Quantitative RT–PCR

P19 cells were cotransfected with UI2-GFP/puro-SIBR vectors (1.5 μg) and US2-Ngn2 or US2-puro (0.5 μg) for 2 μg total DNA per well of a 6-well dish (Costar). The RNA was collected 24 h after transfection and 12 h of puromycin selection (14 μg/ml). RNA was purified using an RNeasy kit (Qiagen) and treated with DNase I (Epicentre). RNA was reverse transcribed using random 12mer primers. cDNA (50 ng) was used per PCR. RNA levels were measured by SYBR green incorporation (ABI SYBR Green PCR master mix) using a BioRad iCycler with MyiQ light module. Primers sequences were obtained from PrimerBank (45) (PrimerBank IDs: RASSF1 13383929a1, HP1γ 6680860a1, NeuroD1 33563268a1, GAPDH 6679937a1 and HPRT 7305155a1). Changes in expression levels were calculated by comparison with serial dilutions of input cDNA for the UI2-puro/GFP-SIBR

Luc-1601 samples. Data presented are averaged from three RNA samples for each vector/condition, assayed using duplicate or triplicate PCR replicates.

Mapping mRNA cleavage sites

RNA-ligase mediated RACE was used to map the internal cleavage sites of target mRNAs (GeneRacer, Invitrogen). Of total RNA isolated for quantitative RT–PCR (qRT–PCR) (above), 5 μg was ligated to an RNA adaptor oligonucleotide. After first strand cDNA synthesis primed with a gene-specific primer, ligation products were PCR amplified with primers complementary to the GeneRacer RNA adaptor and the gene-specific primer. After a second round of PCR with nested primers, PCR products were gel purified and cloned into pCR4-TOPO TA cloning vector for sequencing.

Western blotting

P19 cells were plated to a density of 1.1×10^5 cells per 35 mm dish and transfected ~24 h later using FuGene6. Each transfection contained a total of 4 μg DNA: 3.5 μg UI2-puro vector and 0.5 μg US2-GFP. Puromycin was added (14 μg/ml) 7 h after transfection to select the transfected cells. The puromycin-containing medium was removed 17 h later, and the cells were allowed to recover in MEMα with 2.5% FBS (Hyclone) and 7.5% CS (Hyclone) for an additional 24 h. Extracts were prepared in Triton Immunoprecipitation (TI) buffer (10 mM HEPES, pH 7.4, 150 mM NaCl, 1% Triton X-100, 2 mM EDTA, 0.1% β-mercaptoethanol, 1% aprotinin, 50 mM NaF, 1 mM phenylmethylsulfonyl fluoride). A Bradford dye-binding protocol (BioRad) was used to normalize samples with respect to total protein concentration prior to SDS–PAGE. Primary antibodies for western analyses were α-B-Raf (Santa Cruz sc-166), α-c-Raf (Upstate 05-739) and α-Erk (generous gift of Kun-Liang Guan, University of Michigan). Secondary HRP-antibodies for western analyses were obtained from BioRad. Western blots were developed using SuperSignal West Dura or Pico Chemiluminescence reagents (Pierce). Films (Kodak BioMax MR) were scanned on an Epson Expression 1680 scanner and captured using VueScan 8.1.3.

Immunofluorescence and microscopy

For indirect immunofluorescence, cells were fixed 5 days after transfection and processed as described previously (40). Antibodies used were as follows: rabbit anti-GFP polyclonal antibody diluted 1:2000 (Molecular Probes); mouse monoclonal TuJ1 antibody against neuronal class III β-tubulin diluted 1:2000 (CRP); mouse anti-HP1γ monoclonal antibody diluted 1:1500 (Chemicon); goat anti-rabbit Alexa-488 conjugated secondary antibody and goat anti-mouse Alexa-546 conjugated secondary antibody diluted 1:1000 (Molecular Probes). GFP fluorescence in cells transfected with ubC-driven GFP vectors was photographed in cells fixed 45–48 h after transfection, using a Zeiss Axiovert S100 inverted fluorescence microscope with a DAGE 330 video camera and ImageJ software version 1.34. Image brightness was reduced by 20% and composite images were assembled using Adobe Photoshop 7.0.

RESULTS

To determine if the region of mouse BIC that contains the miR-155 precursor is sufficient for expression of miR-155 in mammalian cells, we inserted a 456 nt fragment from the third exon of mouse BIC (BIC 99–554), including the miR-155 sequence, into the CS2+ expression vector (Figure 1A). The BIC fragment is under the control of the simian CMV IE94 promoter (sCMV) and the SV40 late polyadenylation site is present immediately afterwards. We assessed production of mature miR-155 miRNA using a luciferase reporter construct in which an artificial 22 nt sequence completely complementary to miR-155 was present in the 3′-UTR after luciferase (UAS-luc-miR155as, Figure 1B). Coexpression of miR-155 with the luc-miR-155as reporter should lead to cleavage of the luciferase mRNA by RISC and a consequent reduction in luciferase activity. Cotransfection of mouse P19 cells with the UAS-luc-miR-155as reporter and BIC 99–554 reduced luciferase activity more than 5-fold, relative to cotransfection of the luciferase reporter with a control vector that did not contain BIC sequences, indicating that expression of the mouse BIC third exon fragment is sufficient to produce mature miR-155 (Figure 1C). To delimit the domain of BIC necessary for miR-155 production, we constructed a series of vectors with various deletions within the BIC 99–554 region and tested their ability to inhibit the luciferase reporter in cotransfection assays (Figure 1A and C). The smallest fully functional domain tested contained 108 nt fragment (BIC 134–241). This segment of BIC contains the miR-155 stem–loop precursor and adjacent evolutionarily conserved sequences that can form an extended RNA duplex (35). Further deletion from the 3′ end of this sequence (BIC 134–232 or BIC 99–232) substantially decreased inhibition of the luciferase reporter, suggesting that miR-155 production requires the extended RNA duplex adjacent to the precursor stem–loop, consistent with previous analyses of miRNA primary transcript processing by Drosha (18,46). BIC 134–416 and BIC 134–283 appeared slightly more efficient at reducing luciferase activity than the original BIC 99–554. Expression of BIC 134–283 without the SV40 polyadenylation site (BIC 134–283 ΔpA) also efficiently inhibited luciferase activity, suggesting that efficient polyadenylation is not necessary for miR-155 production. Production of miR-155 was also confirmed by northern blot analysis of RNA collected from transfected cells for a subset of the BIC-derived vectors. A single band of the expected size was detected by a probe complementary to miR-155 for all vectors tested except BIC 134–232 (Figure 1D), consistent with the limited inhibition of the UAS-luc-miR-155as reporter by this vector. The BIC 134–283 ΔpA produced a higher level of mature miR-155 than the other vectors.

We tested whether we could use a BIC-derived vector for RNAi by replacing miR-155 with a synthetic miRNA sequence complementary to a target mRNA. We constructed a variant of the BIC 134–283 vector in which the miR-155 stem–loop precursor could be replaced by insertion of a synthetic 64 nt DNA duplex that encoded a synthetic miRNA (Figure 2). We refer to this synthetic variant of the 134–283 domain of BIC as the SIBR (synthetic inhibitory BIC-derived RNA) cassette. We replaced the miR-155 sequence with either of two 22 nt sequences completely complementary to the 3′-UTR of the mouse neuroD1 mRNA

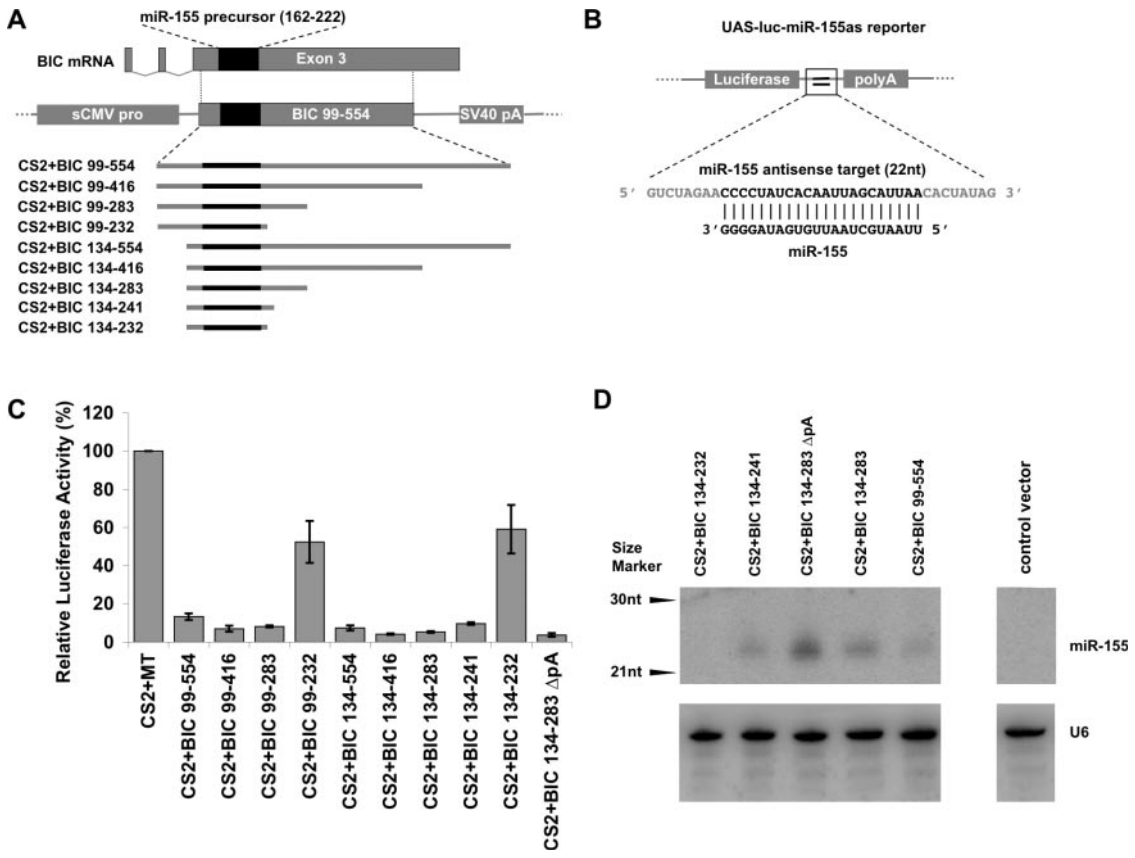

Figure 1. Identification of the minimal region of BIC for miR-155 expression. (**A**) Schematic representation of the mouse BIC non-coding RNA, which contains the miR-155 precursor in the third exon. To express miR-155, 455 nt of the BIC third exon was placed under the control of the sCMV RNA polymerase II promoter, followed by the SV40 late polyadenylation site. Smaller fragments of the third exon (with boundaries based on homologous sequences among human, mouse, and chick BIC RNAs), were used to determine the minimal domain within the third exon of BIC required for miR-155 expression. Positions of starting and ending nucleotides are indicated. Exon and intron sizes are not to scale. (**B**) The UAS-luc-miR-155as reporter contains a single copy of a 22 nt artificial miR-155 target sequence perfectly complementary to miR-155, inserted into the 3′-UTR of the luciferase mRNA. (**C**) Relative luciferase activity after cotransfection of BIC expression vectors with the UAS-luc-miR-155as reporter. CS2+MT, which expresses a multimerized myc-epitope tag, was used as a control. BIC 134–283 ΔpA indicates the BIC 134–283 expression vector with the polyadenylation signal deleted. Standard errors are indicated. (**D**) Upper panel: northern blot for miR-155 in cells transfected with the indicated vectors. The control vector is ND1-1379, in which the miR-155 sequence is replaced with an unrelated sequence (see Figure 2). Lower panel: the same blot re-probed for the U6 snRNA as a loading control.

(SIBR ND1-1379 and SIBR ND1-1888, numbering denotes the position of the first nucleotide in the complementary target sequence). The sequence of the complementary strand in the stem–loop was altered to maintain the RNA duplex. The loop sequence of the BIC/miR-155 precursor, as well as two unpaired nucleotides in the miRNA precursor duplex, were retained in these derivatives (Figure 2). These vectors were expected to produce synthetic 22 nt miRNAs complementary to the NeuroD1 mRNA in mammalian cells. We refer to these synthetic short RNAs here as miRNAs, although they could be considered siRNAs under the current terminology used for RNAi in mammalian cells.

We assessed whether various SIBR vectors (Figure 3A) are functionally effective as RNAi vectors for producing synthetic miRNAs and inhibiting artificial target sequences. First, northern blot analyses using a probe complementary to the introduced miRNA sequences indicated that both the SIBR ND1-1379 and SIBR ND1-1888 vectors produced a single miRNA of the same size as miR-155 in transfected cells (Figure 3B and data not shown). As we observed for miR-155, removal of the SV40 polyadenylation site from the SIBR ND1-1379 vector (Figure 3A: ND1-1379 ΔpA) increased the level of the ND1-1379 miRNA (Figure 3B). In a reporter assay, either of the SIBR ND1 vectors effectively reduced luciferase activity when cotransfected with a reporter construct that expressed an mRNA for the luciferase coding region followed by the mouse NeuroD1 3′-UTR (UAS-luc-ND1-UTR) (Figure 3C). Activity of the reporter was not reduced by cotransfection of the BIC 134–283 vector, indicating that inhibition was dependent on the synthetic NeuroD1-complementary miRNA sequences in the SIBR cassette. A luciferase reporter that contained a sequence complementary to the second strand of the stem–loop in the ND1-1379 SIBR cassette was inhibited <2-fold (data not shown), indicating that the NeuroD1-complementary first strand is likely to preferentially accumulate in the cell as the functional miRNA.

We tested whether two different miRNAs could be produced from a single transcription unit using the BIC-derived sequences. The NeuroD1-1379 SIBR cassette and the BIC 134–283 fragment were inserted in tandem into the CS2+ vector (Figure 3A: SIBR ND1-1379 + BIC 134–283).

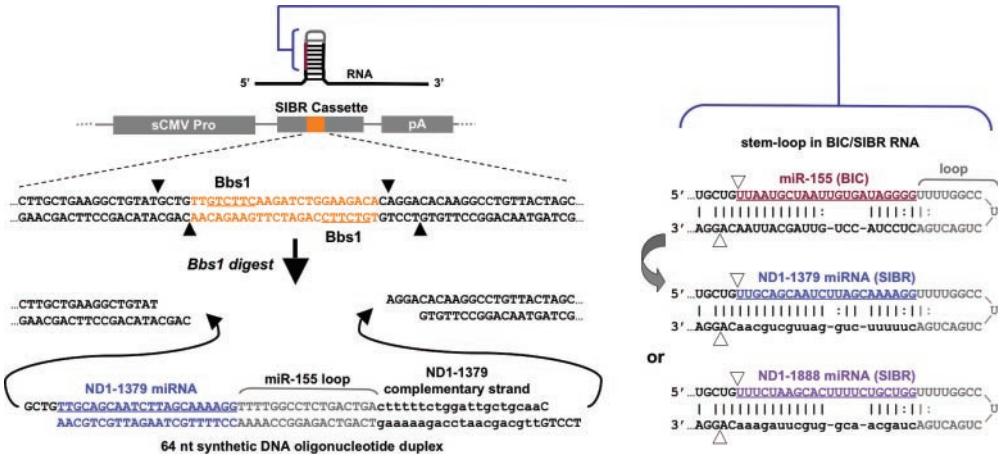

Figure 2. RNAi vectors based on the miR-155 primary transcript BIC. The SIBR cassette was constructed by replacing the miR-155 precursor stem–loop in the BIC 134–283 fragment with a polylinker (orange) containing inverted Bbs1 restriction sites. The Bbs1 cut sites (filled triangles) are outside the recognition sites (underlined). A synthetic 64 nt DNA duplex can be inserted in which the miR-155 miRNA sequence is replaced by a synthetic miRNA sequence (blue). The primary RNA transcript from the SIBR vector is indicated above the schematic, with the miRNA containing stem–loop indicated and shown in more detail on the right. The stem–loop in the primary RNA is processed by Drosha to release a stem–loop pre-miRNA, which is then processed by Dicer to release the mature miRNA. Expected Drosha cleavage sites are indicated by open triangles. Each mature miRNA is underlined. The miR-155 sequence in the stem–loop of the BIC RNA (red) is replaced by either of two synthetic miRNA sequences (blue or purple) perfectly complementary to the 3′-UTR of the mouse NeuroD1 mRNA (ND1). The complementary strand of the stem–loops for the ND1 miRNAs was altered to maintain a partial duplex with two single base gaps (lower case). The loop (grey) and flanking sequences (upper case black) are from BIC. Numbers for synthetic miRNAs indicate the first nucleotide of the target mRNA that is complementary to the miRNA.

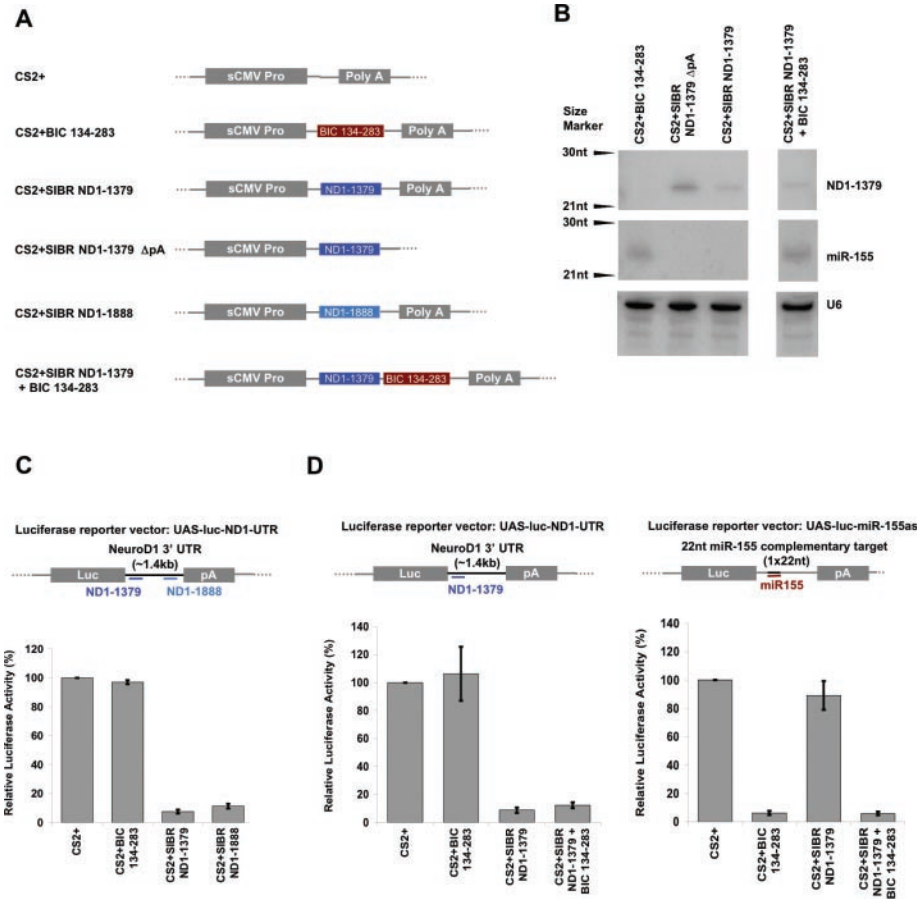

Figure 3. Sequence specific inhibition by SIBR vectors. (**A**) Schematic diagrams of variants of SIBR expression vectors with single or tandem cassettes. (**B**) miR-155 and the ND1-1379 synthetic miRNA are detected as single bands and at similar levels by northern blot analysis of RNA from P19 cells transfected with single and tandem SIBR vectors. Deletion of the polyadenylation signal (ND1-1379 ΔpA) increased the level of ND1-1379 miRNA. Bottom panel: the same blot re-probed for the U6 snRNA as a loading control. (**C**) Cotransfection of SIBR vectors expressing miRNAs complementary to NeuroD inhibit a cotransfected luciferase reporter containing the mouse NeuroD1 3′-UTR, while BIC 134–283 has no effect on luciferase activity. (**D**) A vector with both a ND1-1379 SIBR cassette and BIC 134–283 in tandem effectively inhibits a luciferase reporter for either miRNA. The level of inhibition from the tandem vector is comparable with that of the individual vectors. Standard errors are indicated.

In northern blot analyses, the SIBR ND1-1379 + BIC 134–283 vector produced both the ND1-1379 miRNA and the miR-155 miRNA at levels similar to the individual vectors (Figure 3B, right panel). Also, the SIBR ND1-1379 + BIC 134–283 vector inhibited both the UAS-luc-miR-155as and UAS-luc-ND1-UTR reporters in cotransfection assays (Figure 3D). Inhibition by the tandem SIBR cassette vector in this assay was as effective as inhibition by either the BIC 134–283 or ND1-1379 SIBR vector. A control luciferase reporter that lacked target sequences for both miR-155 and ND1-1379 was not inhibited by cotransfection of BIC 134–283, SIBR ND1-1379 or SIBR ND1-1379 + BIC 134–283 (data not shown).

Since the SIBR cassette can be expressed using a RNA polymerase II transcript, we were interested in developing a vector that could express both a protein (e.g. a visible or selectable marker) and one or more SIBR cassettes from a single transcription unit. Some endogenous miRNAs are located in the introns of protein coding genes and at least some of these intronic miRNAs are coexpressed with the corresponding mature mRNA, suggesting that an miRNA precursor can be processed from an intron without preventing mRNA accumulation (22). We constructed a derivative of the CS2 vector, US2, in which the simian CMV IE94 promoter was replaced by the human ubC promoter and first intron (43,47). The US2 vector was modified to include the SIBR cassette within the ubC intron, followed by an exon that encoded either GFP or the puromycin resistance protein (designated UI2-GFP-SIBR and UI2-puro-SIBR respectively) (Figure 4A). We compared inhibition by the SIBR ND1-1888 cassette expressed in each of these vectors, using the UAS-luc-ND1-UTR reporter in cotransfection assays. For the CS2 and US2 vectors, a derivative that did not include a polyadenylation site was used, since inhibition with these vectors was more effective when the polyadenylation site was removed (Figures 1 and 3; data not shown). All four vectors provided comparable inhibition of the reporter (Figure 4B), indicating that the SIBR cassette is effectively expressed when located within the ubC intron. Expression of GFP was not appreciably altered by the presence of the SIBR cassette in the UI2-GFP intron (Figure 4C).

We have constructed SIBR vectors that target a variety of different mRNAs (Table 1). Target sequences for miRNAs were chosen using previously described rules for siRNA target selection (48) and the additional constraint that the first base of the miRNA should be a U or an A. The miR-155 strand in the mouse, human and chicken miR-155 stem–loop precursors is two bases longer than its complementary strand, leading to the presence of unpaired bases in the miRNA precursor duplex. We have maintained the two base length difference between the two strands in the synthetic constructs used here, and if possible chose sequences that led to structures similar to the native miR-155 precursors. For example, ND1-1888 has a duplex similar to the mouse miR-155 precursor, ND1-380 has a duplex similar to the human miR-155 precursor, and the Luc-1601 precursor has a duplex structure like the chicken miR-155 precursor. However, some sequences preferentially fold into alternate structures when two bases are removed from the complementary strand, such that some effective SIBR miRNA precursors have predicted duplex structures that differ from all three miR-155 miRNA precursors (e.g. HP1γ-664 and

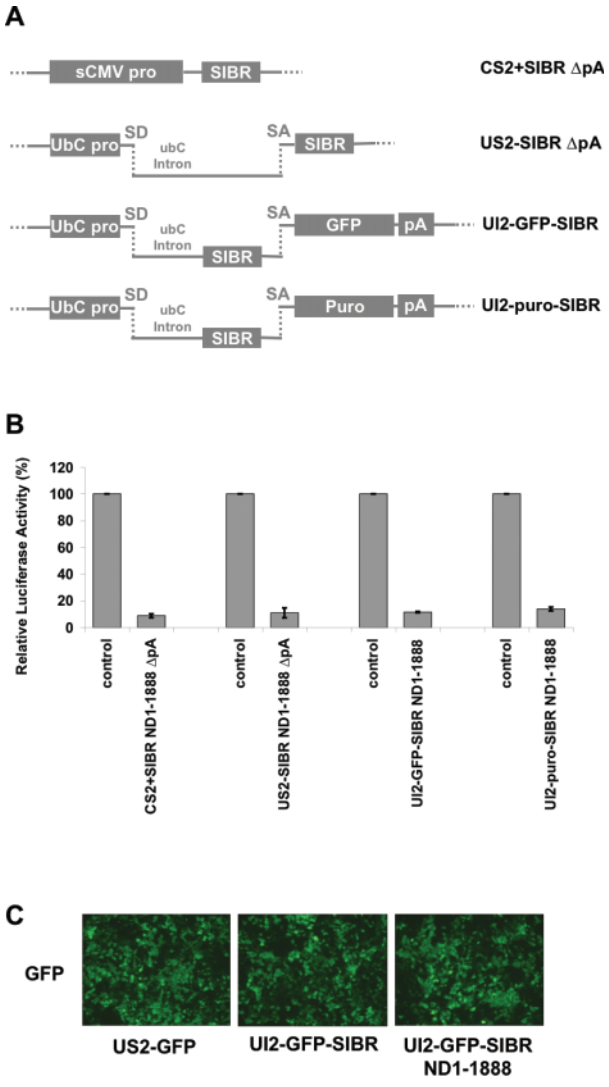

Figure 4. Expression of the SIBR cassette from an intron. (**A**) Schematic diagrams of SIBR vectors: US2-SIBR ΔpA vector contains the SIBR cassette in the second exon of human ubC gene, under control of the human ubC promoter, but without a polyA signal. There is no coding region present in either the CS2+SIBR ΔpA or US2-SIBR ΔpA vector. UI2 vectors also use the human ubC promoter but contain the SIBR cassette in the first intron of the ubC gene, with the GFP or puromycin-resistance proteins expressed from the second exon. SD and SA indicate splice donor and splice acceptor, respectively. Exon and intron sizes not to scale. (**B**) Different SIBR vector designs expressing the ND1-1888 miRNA against NeuroD1 were cotransfected with the NeuroD1 3′-UTR luciferase reporter (see Figure 2). All four designs with ND1-1888 showed similar levels of inhibition of the reporter. Control SIBR vectors used the same designs but expressed an unrelated miRNA directed against the mouse POSH mRNA. Standard errors are indicated. (**C**) Comparable GFP fluorescence was detected 24 h after transfection with GFP expressed from ubC-based expression vectors, whether or not a functional SIBR cassette was present in the ubC intron.

c-Raf-2268). When compatible with the synthetic miRNA sequence, we included GU base pairs between the miRNA and its complement at the same positions that GU basepairs are found in the miR-155 stem–loop precursor. However, the GU base pairs are not essential for function (e.g. GAPDH-528 and Luc-1601 have none).

To determine the effectiveness of the SIBR vectors for inhibiting endogenous mRNAs, we tested the ability of the

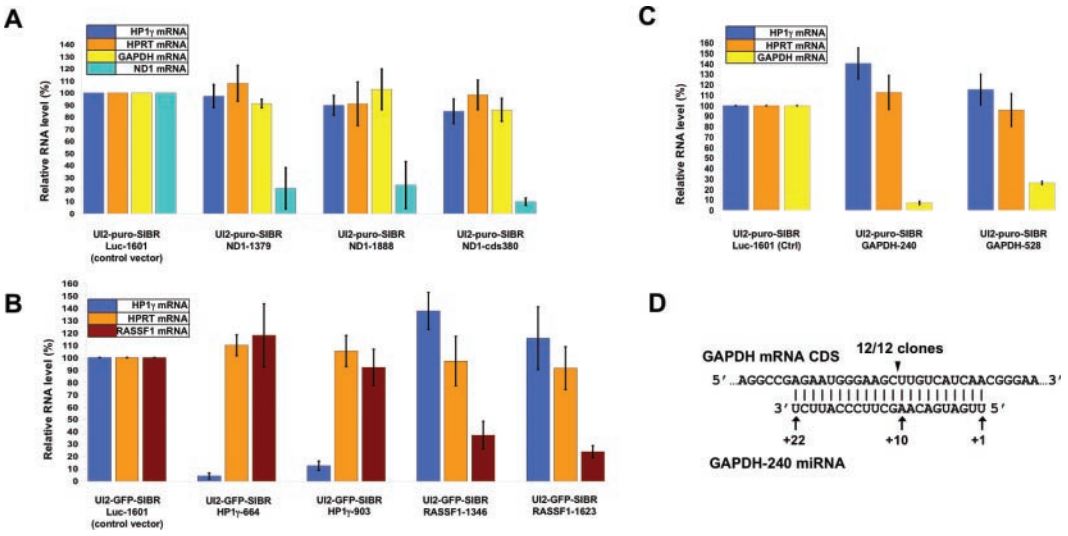

Figure 5. Knock-down of endogenous genes using UI2 SIBR vectors. (**A**) qRT–PCR measurements of mRNA levels in P19 cells transiently cotransfected with an expression vector for Ngn2 (to activate endogenous NeuroD1 expression), and various UI2-puro-SIBR vectors. The level of NeuroD1 mRNA was reduced by miRNAs directed against the NeuroD1 3′-UTR (see Figure 2) or coding region (ND1-380), but not by a control miRNA directed against Luciferase. GAPDH and HPRT mRNA levels were not reduced. (**B**) UI2-GFP-SIBR vectors expressing miRNAs that target the HP1γ or RASSF1 mRNAs reduced the levels of the corresponding endogenous mRNA in transfected P19 cells, but not the HPRT mRNA. (**C**) UI2-puro-SIBR vectors expressing miRNAs directed against GAPDH reduce endogenous GAPDH mRNA levels. (**D**) Expression of the GAPDH-240 miRNA leads to cleavage of the endogenous GAPDH mRNA at the expected site (see text). In A–D, transfected cells were selected with puromycin to remove untransfected cells. UI2-GFP-SIBR vectors in B were cotransfected with US2-puro to permit selection.

ND1-1379 and ND1-1888 SIBR cassettes to reduce the level of the NeuroD1 mRNA. P19 cells were cotransfected with a UI2-puro-SIBR vector and a US2 expression vector for the mouse neurogenin2 bHLH protein (Ngn2) to activate endogenous NeuroD1 expression (40). Transiently transfected cells were selected with puromycin to remove untransfected cells (25). The level of NeuroD1 mRNA was measured by qRT–PCR (Figure 5A). Both the ND1-1379 and the ND1-1888 vectors reduced NeuroD1 mRNA levels about 5-fold, relative to a control SIBR vector directed against luciferase, while ND1-380, a SIBR vector directed against a sequence in the NeuroD1 coding region was more effective, reducing the NeuroD1 mRNA by about 10-fold. The levels of mRNAs from three unrelated genes, hypoxanthine ribosyltransferase (HPRT), glyceraldehyde-3-phosphate dehydrogenase (GAPDH) and the chromatin protein HP1γ, were not affected, indicating that inhibition of NeuroD1 by the SIBR vectors was specific. We tested SIBR cassettes that target additional endogenous genes using the UI2-GFP and UI2-puro vectors, including HP1γ, the tumor suppressor RASSF1 and GAPDH. Vectors were tested in transiently transfected cells, with puromycin selection after transfection. As controls for non-specific effects, UI2-GFP and UI2-puro SIBR vectors directed against luciferase were used. Both vectors that targeted HP1γ substantially reduced HP1γ mRNA levels, in one case nearly 30-fold (Figure 5B). The SIBR vectors directed against RASSF1 were somewhat less effective, reducing RASSF1 mRNA 3- to 5-fold (Figure 5B). Both vectors for GAPDH reduced mRNA levels, with the more effective vector reducing levels by about 10-fold (GAPDH-240, Figure 5C). In all cases, the SIBR vectors did not decrease the expression of non-targeted mRNAs (Figure 5A–C).

Previous studies have shown that the RISC complex cleaves mRNAs between the target mRNA bases complementary to the 10th and 11th nucleotides of a perfectly complementary siRNA/miRNA (7,49). We used ligation-mediated RT–PCR to identify the location of the 5′ end of the 3′ fragment from the cleaved GAPDH mRNA in cells transfected with the GAPDH-240 SIBR vector (9,50). All 12 clones sequenced had the expected 5′ end for the predicted cleavage product (Figure 5D). This observation indicates that the SIBR vector derived miRNAs function by RISC-mediated cleavage of the target mRNA as expected and confirms that the 5′ end of the synthetic miRNA is at the expected position. We also observed HP1γ mRNA cleavage products with the expected 5′ end in RNA isolated from cells transfected with UI2-GFP-SIBR HP1γ-664 (data not shown).

One potential application of the UI2-GFP-SIBR vectors is RNAi analysis using individual identified cells. We transiently transfected cells with UI2-GFP-SIBR HP1γ-664 or UI2-GFP-SIBR luc-1601. Cells were fixed and processed for indirect immunofluorescence to detect GFP and the endogenous HP1γ protein (Figure 6). UI2-GFP-SIBR HP1γ-664 transfected cells that expressed GFP had low or undetectable HP1γ signals, while untransfected cells or the cells transfected with the UI2-GFP-SIBR luc-1601 vector had strong HP1γ signals. For the cells transfected with the UI2-GFP-SIBR luc-1601 control vector, 96% of the GFP positive cells were strongly positive for HP1γ ($n = 110$ cells). For the cells transfected with UI2-GFP-SIBR HP1γ-664, only 4% of the GFP positive cells were strongly positive for HP1γ ($n = 158$ cells). These observations indicate that there is efficient coexpression of the synthetic miRNA and the GFP marker at the single cell level.

We also compared the inhibitory efficiency of SIBR vector with a previously described RNA polymerase III driven shRNA vector for the same target mRNA. The U6-Tubb3HP2 vector (originally named U6-BT4HP2) expresses an effective

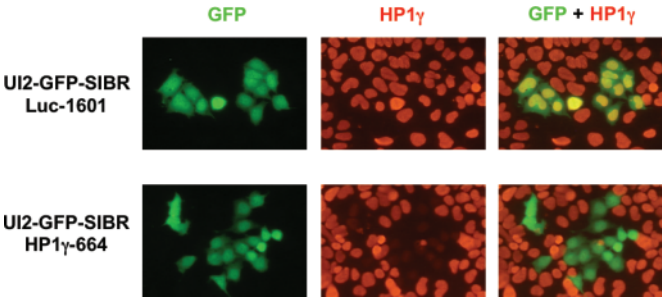

Figure 6. Reduction of endogenous HP1γ protein in single cells identified by coexpressed GFP. P19 cells transfected with the UI2-GFP-SIBR HP1γ-664 vector express GFP (green) and show reduced HP1γ by indirect immunfluorescence (red) when compared with untransfected cells (no GFP). The HP1γ signal in cells transfected with the UI2-GFP-luc1601 control vector remains unchanged.

shRNA directed against the 3′-UTR of mouse tubulin β3 (Tubb3), under the control of the mouse U6 promoter (24,51). We constructed a vector directed against mouse tubulin β3 (UI2-GFP-SIBR Tubb3-1549) that targets a sequence overlapping the target site of the U6-Tubb3HP2 shRNA vector. U6 or SIBR vectors were cotransfected with a reporter construct that contains the 3′-UTR of mouse tubulin β3 inserted after the luciferase coding region. In a luciferase reporter assay, the UI2-GFP-SIBR vector reduced luciferase activity as effectively as the U6 vector at three different plasmid amounts (Figure 7A). We also transiently cotransfected P19 cells with U6 or UI2-GFP-SIBR vectors directed against tubulin β3, or control SIBR vectors, and the US2-Ngn2 vector to activate neuronal differentiation (40). An additional UI2-GFP-SIBR vector which targets a different sequence in the tubulin β3 3′-UTR was also tested. After four days of differentiation in culture, endogenous tubulin β3 expression was detected by indirect immunofluorescence. Most cells transfected with U6-Tubb3HP2, UI2-GFP-SIBR Tubb3-1549 or UI2-GFP-SIBR Tubb3-1512 vectors showed substantially reduced or undetectable tubulin β3 protein expression in cell bodies and neurites when compared with cells tranfected with the control vectors (Figure 7B).

As described above, both miR-155 and a SIBR cassette can be expressed from a single transcription unit. The CS2+SIBR and UI2-SIBR vectors were designed to facilitate multimerizing the SIBR cassette by providing unique but compatible restriction sites flanking the cassette (Figure 8A and B). To determine if a tandem SIBR vector can be used to inhibit two endogenous mRNAs, we constructed SIBR vectors that specifically targeted the related kinases B-Raf and c-Raf. An effective SIBR cassette against each kinase was inserted individually or in tandem into the intron of the UI2-puro-SIBR vector (Figure 8C). Transient transfection of SIBR vectors against either c-Raf or B-Raf effectively and specifically reduced the level of the targeted Raf protein, but not the untargeted Raf kinase, while the tandem B-Raf + c-Raf SIBR vector reduced the levels of both proteins (Figure 8D). The level of the downstream kinase ERK, which was not targeted, remained unchanged.

The ability to effectively express two synthetic miRNAs from a single transcript raised the possibility that including more than one copy of a miRNA against the same target mRNA in a single SIBR vector might improve inhibition of the target. We compared the UI2-GFP vector with two to eight tandem SIBR cassettes, each containing the same miRNA directed against luciferase, with UI2-GFP vector with a single copy of the same SIBR cassette (Figure 9A). Inhibition of the reporter increased with the number of SIBR cassettes, at three different DNA concentrations, and the vector with eight copies was the most effective (Figure 9B). The UI2-GFP-SIBR vector containing a single copy of an effective miRNA against the unrelated gene POSH (C. Figueroa, K.-H. Chung, J. Taylor, M. Deo, E.J. Brace, A.W. Avery, D.L. Turner and A.B. Vojtek, manuscript submitted) was used as a control. A vector with eight copies of the miRNA against POSH did not alter luciferase expression relative to the control, indicating that a multimerized SIBR cassette did not have a non-specific effect on luciferase expression.

Serendipitously, we observed that expression of an intronic SIBR cassette from a two intron expression vector enhanced target inhibition relative to the UI2-SIBR single intron vectors. A vector was constructed in which the SIBR cassette is located in an intron from the rabbit globin gene, inserted into a modified UI2 vector after the existing ubC intron (UI4-GFP-SIBR vector, Figure 9C). When tested in a cotransfection reporter assay at three different DNA concentrations, the UI4-GFP-SIBR luc-1601 vector showed consistently better inhibition of luciferase than the UI2-GFP-SIBR luc-1601 vector (Figure 9D). Inhibition by the UI4-GFP SIBR luc-1601 vector was approximately the same as the level of inhibition by a UI2-GFP-SIBR luc-1601×2 vector that has two copies of the luc-1601 SIBR cassette. Including two copies of the luc-1601 SIBR cassette in the UI4-GFP-SIBR vector increased inhibition relative to a single copy of the SIBR cassette, indicating that multimerization of the SIBR cassette can be used to further enhance inhibition with the UI4-GFP-SIBR vector (Figure 9D). To test whether the enhanced inhibition was specific to the expression of the SIBR cassette from the rabbit globin intron, we constructed a single intron vector similar to UI2-GFP-SIBR in which the ubC intron was replaced with the rabbit globin intron/SIBR cassette (still driven by the ubC promoter). That vector provided target inhibition similar to UI2-GFP-SIBR (data not shown), suggesting that the enhanced inhibition with UI4-GFP-SIBR is a result of having two introns present in the transcript or expressing the SIBR cassette from the second intron, rather than a function of the specific intronic sequences that flank the SIBR cassette.

DISCUSSION

Vector-based RNAi has become a popular approach for analyzing gene function in mammalian cells. We describe here a new RNA polymerase II vector system for RNAi, the SIBR vectors, based on BIC, the primary transcript for the miR-155 miRNA. The SIBR vectors produce a synthetic miRNA, perfectly complementary to a target mRNA, leading to target mRNA cleavage. RNA polymerase II vectors based on production of a synthetic miRNA from a modified miR-30 miRNA precursor, were first described and characterized by Cullen and colleagues (8,27,28). Optimized RNAi vector designs based upon miR-30 have been described recently and have been adapted for use in RNAi libraries (31,32,52). Both the miR-155 based SIBR vectors and recent miR-30

based designs provide similar levels of inhibition to RNA polymerase III shRNA vectors. However, in contrast to previously described miR-30 based or shRNA vectors, we show that the SIBR vectors can be used to express multiple miRNA expression cassettes from a single transcript. Two different synthetic miRNAs directed against two different target mRNAs can be expressed from a single polycistronic transcript containing two SIBR cassettes, and both miRNAs provide effective RNAi. Alternately, multimerization of a single miRNA cassette up to at least eight copies can be used to increase the inhibition of a single target mRNA. We also find that expression of an intronic SIBR cassette from a two intron vector enhances inhibition, and this design can be combined with multimerization of the SIBR cassettes.

Although synthesis of multiple endogenous miRNAs from polycistronic transcripts has been reported (16,20,21), effective vectors for RNAi that can target more than one mRNA using a single transcription unit have not been described. Cullen and colleagues demonstrated coexpression of a synthetic miRNA and the natural miR-30 miRNA from a single transcript using an expression vector (53), but they did not test whether two synthetic miRNAs could be used for effective target inhibition by RNAi. Zhou *et al*. reported that expressing two tandem copies of a miR-30-based synthetic miRNA in a single transcription unit was less effective for RNAi than a single copy of the same miRNA (29). That observation raised the possibility that the inclusion of two or more miRNAs in a transcript might reduce the amount of each mature miRNA produced: processing of one miRNA could potentially destabilize the transcript or otherwise interfere with the subsequent processing of other miRNAs from the same transcript. Such problems would reduce the utility of polycistronic vectors for RNAi. However, we show that tandem expression cassettes for two different miR-155-based synthetic miRNAs can be expressed in a single transcription unit, and each miRNA functions for RNAi with an efficiency similar to that of a single miRNA expression vector. We also found that the SIBR expression cassette for a single miRNA could be multimerized in tandem, up to at least eight copies, resulting in increased target inhibition. The reason for the difference between the miR-30 and the BIC/miR-155 based vectors in polycistronic transcripts is not clear. Possibly tandem copies of the miR-30 derived stem–loop folded into an unexpected structure; alternately, BIC-derived sequences might stabilize a partially processed pri-miRNA transcript or otherwise facilitate generation of pre-miRNAs by Drosha.

An advantage of RNA polymerase II based RNAi vectors is the ability to coexpress a synthetic miRNA and a protein marker from a single transcription unit. Cullen and colleagues demonstrated that a miRNA could be expressed from the

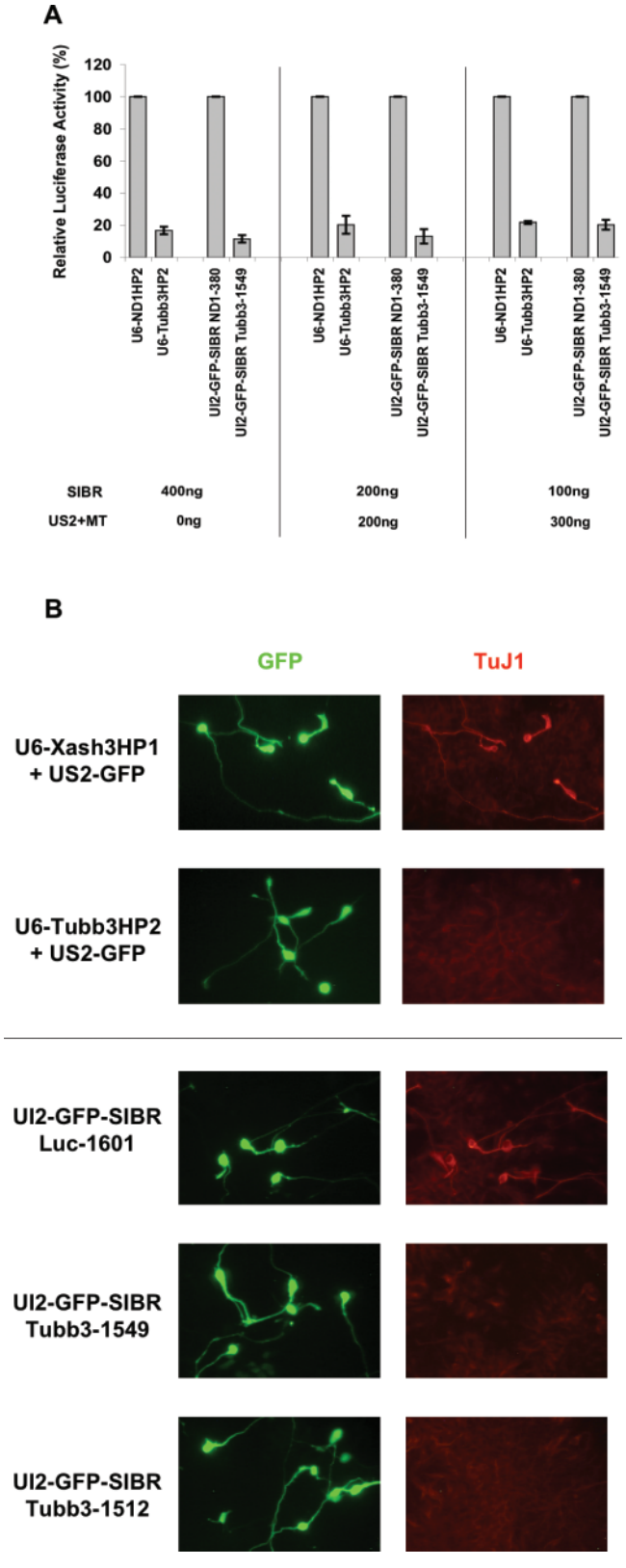

Figure 7. Comparable inhibition by SIBR vectors and a U6 shRNA vector. (**A**) A reporter assay comparing inhibition of a luciferase reporter containing 3′-UTR of mouse tubulin β3 (luc-Tubb3-UTR) cotransfected with either the UI2-GFP-SIBR Tubb3-1549 vector or the U6-Tubb3HP2 vector. At three different plasmid concentrations, both vectors showed comparable levels of inhibition. Standard errors are indicated. (**B**) Reduction of endogenous mouse tubulin β3 protein at a single cell level demonstrated by immunocytochemistry. U6 or UI2-GFP-SIBR vectors were cotransfected into P19 cells together with the US2-Ngn2 vector to induce neuronal differentiation and β3 tubulin expression. U6 transfections included the US2-GFP vector to label transfected cells. P19 cells transfected with a U6 shRNA vector or either of two UI2-GFP-SIBR vectors (green) directed against β3 tubulin showed substantially reduced tubulin β3 protein (red) by indirect immunfluorescence, relative to cells transfected with control vectors.

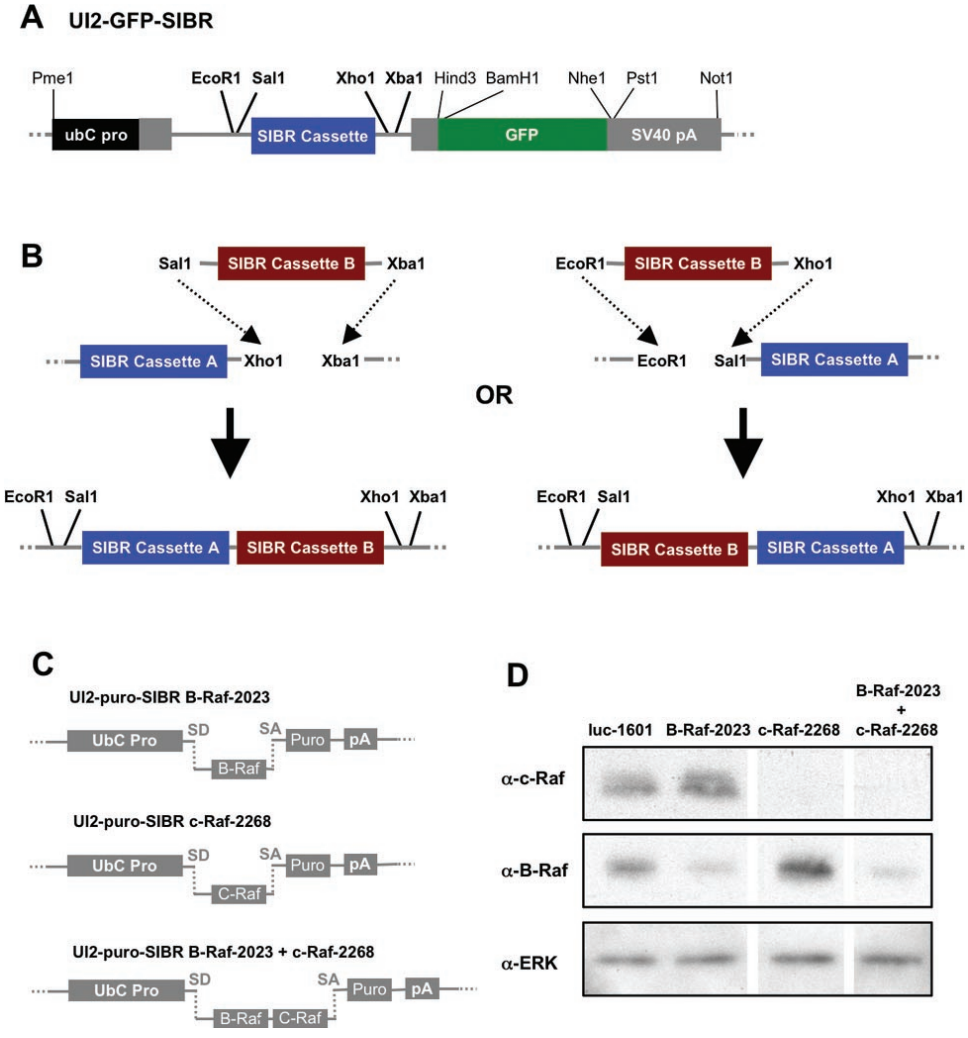

Figure 8. Knock-down of two endogenous genes using a single UI2 SIBR vector. (**A**) Schematic of the UI2-GFP/puro-SIBR vectors showing unique restriction sites flanking the SIBR cassette. Indicated in bold are restriction enzyme sites used for multiplexing SIBR cassettes. (**B**) Using appropriate restriction enzymes, it is possible to create vectors with tandem SIBR cassettes rapidly. (**C**) Schematic of vectors with miRNAs directed against the B-Raf and/or c-Raf kinases, including a vector with tandem B-Raf and c-Raf SIBR cassettes. Schematics in **A-C** are not to scale. (**D**) Western blot showing reduced levels of either B-Raf or c-Raf protein in cells transfected with SIBR vectors expressing a miRNA against the corresponding mRNA, but not in cells transfected with a control vector expressing a miRNA directed against luciferase. The vector expressing two miRNAs targeting the B-Raf and c-Raf mRNAs reduced the levels of both Raf proteins, but not the ERK kinase.

3′-UTR of a luciferase expression vector, although they did not describe a vector of this design for RNAi (17). The miR-155 precursor stem–loop is located in an exon, but we found that an intronic SIBR cassette could be used to effectively express a synthetic miRNA, while the mature mRNA from the same transcription unit could encode a protein marker. Zhou *et al*. described an RNAi vector in which a synthetic miRNA derived from the miR-30-based precursor is expressed from the intron of a protein marker gene under the control of the human ubC promoter, using a vector design similar to our UI2-GFP-SIBR vector (29). Additional RNAi vector designs for coexpression of a protein and an shRNA recently have been reported (54–56). We also observed that an intronic SIBR cassette from the two intron UI4-GFP-SIBR vector increased RNAi relative to the single intron UI2-GFP-SIBR vector. The reason for the increased inhibition with the two intron vector is unclear. Removal of the polyA signal from an unspliced transcript with a SIBR cassette increased the level of the mature miRNA and led to inhibition at a similar level to a single intron vector. Possibly increased nuclear retention of intronic and non-polyadenylated sequences (57) facilitates processing of miRNA primary transcripts (19). Several endogenous miRNA primary transcripts, including the BIC RNA, have been reported to be retained in the nucleus (17,58).

miR-155 is derived from the non-coding RNA BIC (37,38,58). BIC was originally isolated based on its association with lymphoma in chickens, and its minimal functional domain contains the miR-155 precursor stem–loop (39). Our data indicate that expression of a 108 nt fragment located within the third exon of mouse BIC is sufficient to produce miR-155, consistent with the observation that the third exon of human BIC is sufficient for miR-155 expression (58). The minimal fragment of BIC required for miR-155 expression contains both the predicted miR-155 precursor and adjacent flanking sequences that form an extended RNA duplex (35).

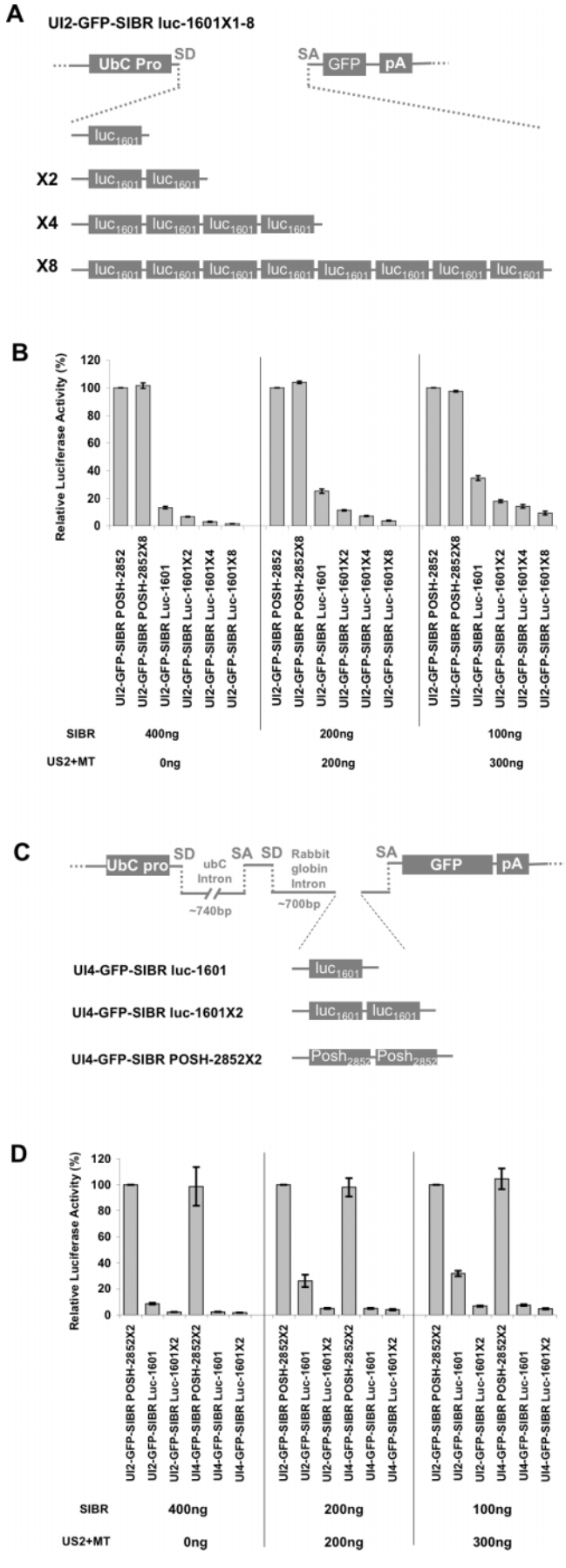

An RNA duplex adjacent to a miRNA stem–loop precursor is essential for efficient Drosha processing (46). The BIC sequences we have used in the SIBR vectors are slightly larger than the minimal domain required for miR-155 production, extending an additional 42 nt on the 3′ side. While not essential, expression of synthetic miRNAs was more consistent among different vector designs when the 3′ extension was included (unpublished observations). The sequence of the 3′ extension is highly conserved in mouse, human and chicken BIC. Possibly, it contributes a structural feature that improves Drosha recognition (59).

To produce synthetic miRNAs, we replaced both miR-155 and its complementary strand within the miR-155 precursor. We retained the unmodified miR-155 loop between these sequences, since the loop sequences are likely to be required for efficient nuclear export of the miRNA precursor (60). We used standard siRNA design rules, adjusted for the 22 nt length of the miRNA, to select miRNA target sequences (48). When possible, we incorporated structural features from the miR-155 precursor into the precursors for synthetic miRNAs. The miRNA containing strand in the chicken, mouse and human miR-155 precursors is 2 nt longer than its complementary strand, although the precursors from each species accommodate the extra nucleotides with slightly different structures (35). We removed two bases on the strand complementary to the synthetic miRNA to create miRNA precursors with a predicted structure similar to the miR-155 precursors. While SIBR constructs in which the two strands are the same length also function, they are less effective in some cases (K.-H. Chung, data not shown). Similarly, Zhou *et al*. observed that synthetic derivatives of the miR-30 precursor that were not completely duplexed increased RNAi relative to a perfect duplex (29). It is not possible to maintain the miR-155-like structure/basepairing for all synthetic precursor sequences, as some sequences fold into alternate structures when two bases are removed. We also included GU base pairs between the synthetic miRNA and its complement at positions where GU base pairs are found in the miR-155 precursor when possible. SIBR vectors with several different predicted precursor duplex structures and different numbers of GU basepairs were effective for RNAi, indicating that the precise duplex structure is

Figure 9. Increased inhibition by multiple SIBR cassettes expressed from a single intron vector, and by use of a two intron vector. (**A**) Schematic representation of UI2-GFP-SIBR vectors expressing one to eight tandem copies of the same synthetic miRNA against luciferase. (**B**) P19 Cells transfected with a fixed amount of target luciferase reporter and a fixed total amount of DNA show dose dependent inhibition of luciferase. At three different DNA concentrations, an increased number of copies of the luc-1601 SIBR cassette in the UI2-GFP vector provided better inhibition. The UI2-GFP-SIBR POSH-2852 control vector expresses a functional synthetic miRNA directed against the mouse POSH gene. A vector with eight copies of the POSH miRNA does not inhibit luciferase. Total DNA amount was kept constant by replacing the SIBR vector with the US2-MT vector, which does not express a miRNA. Standard errors are indicated. (**C**) Schematics of the two intron UI4-GFP-SIBR vectors. UI4-GFP vectors contain the SIBR cassettes in rabbit globin intron, inserted between the exon 2 and GFP in exon 3. Exons 1 and 2 are noncoding. SD and SA indicate splice donor and splice acceptor, respectively. Approximate intron size is indicated. (**D**) Cotransfection reporter assay comparing the inhibition by UI4-GFP-SIBR vectors to UI2-GFP-SIBR vectors expressing one or two miRNAs against luciferase. At three different plasmid concentrations, the UI4-GFP-SIBR vectors showed increased inhibition of luciferase relative to the UI2-GFP-SIBR vectors. Standard errors are indicated.

not crucial. It remains possible that different duplex structures could have subtle effects on processing or other aspects of miRNA production and subsequent RNAi. Other aspects of the miRNA precursor structure may also influence processing. The 2 nt CA 3′ overhang expected for the miR-155/SIBR precursor is the optimal overhang sequence for Dicer processing (61), which may contribute to the effectiveness of the SIBR vectors.

Partial functional redundancy among related genes frequently complicates functional analysis of individual genes. We expect that the SIBR vectors will facilitate the analysis of combinations of genes by RNAi. The vectors allow rapid construction of designs expressing individual miRNAs, and SIBR cassettes expressing single miRNAs can be readily combined into tandem designs. Although the SIBR vectors tested here expressed only two different miRNAs, vectors with four or eight copies of the SIBR cassette provided enhanced target inhibition, suggesting that SIBR vectors directed against more than two targets are possible. In addition, synthesis of the miRNA(s) and a marker protein as a single transcript facilitates the identification or selection of cells expressing the miRNA(s). Alternately, expression of a biologically active protein could be combined with RNAi, e.g. to allow functional analyses of a pathway downstream from the active protein. Both the miRNA processing machinery and RISC appear to be ubiquitous (3). We find that the SIBR vectors function effectively in a variety of mouse, rat and human cell lines (K.-H. Chung, P. Patel and D.L. Turner, unpublished data), and the vectors have been effective for functional analyses of genes in primary mouse neural progenitors and differentiating neurons (C. Figueroa, K.-H. Chung, J. Taylor, M. Deo, E.J. Brace, A.W. Avery, D.L. Turner and A.B. Vojtek, manuscript submitted). In addition to cell culture studies, *in vivo* analyses of redundant gene function in identified cells should be feasible using SIBR vectors delivered by electroporation (43).

ACKNOWLEDGEMENTS

The authors thank Jenn-Yah Yu for helpful discussions, and Takahiko Matsuda and Connie Cepko for providing plasmids. The authors also thank Melissa Tippens for helping to set up small RNA northern blots, and Paul Good and David Engelke for the U6 probe and advice on northern blots. The authors gratefully acknowledge Lawrence Tsoi for assistance with constructing the multimerized SIBR luc vectors. This work was supported by NIMH MH073085 (A.B.V.), American Cancer Society (Research Scholar Grant RSG-01-177-01-MGO, A.B.V.), NIMH MH063992 (P.D.P.), NIH NS38698 (D.L.T.), the University of Michigan Center for Gene Therapy (D.L.T.), and the Wilson Medical Research Foundation (D.L.T.). Funding to pay the Open Access publication charges for this article was provided by the NIH and the University of Michigan.

Conflict of interest statement. The University of Michigan has patents pending on miR-155 based RNAi technology. Kwan-Ho Chung, Paresh Patel, Anne B. Vojtek and David L. Turner are potential recipients of royalties paid to the University of Michigan for licensed use.

REFERENCES

1. Filipowicz,W. (2005) RNAi: the nuts and bolts of the RISC machine. *Cell*, **122**, 17–20.
2. Sandy,P., Ventura,A. and Jacks,T. (2005) Mammalian RNAi: a practical guide. *Biotechniques*, **39**, 215–224.
3. Murchison,E.P. and Hannon,G.J. (2004) miRNAs on the move: miRNA biogenesis and the RNAi machinery. *Curr. Opin. Cell Biol.*, **16**, 223–229.
4. Lagos-Quintana,M., Rauhut,R., Lendeckel,W. and Tuschl,T. (2001) identification of novel genes coding for small expressed RNAs. *Science*, **294**, 853–858.
5. Lau,N.C., Lim le,E.P., Weinstein,E.G. and Bartel da,V.P. (2001) An abundant class of tiny RNAs with probable regulatory roles in *Caenorhabditis elegans*. *Science*, **294**, 858–862.
6. Lee,R.C. and Ambros,V. (2001) An extensive class of small RNAs in *Caenorhabditis elegans*. *Science*, **294**, 862–864.
7. Hutvagner,G. and Zamore,P.D. (2002) A MicroRNA in a multiple-turnover RNAi enzyme complex. *Science*, **1**, 1.
8. Zeng,Y., Yi,R. and Cullen,B.R. (2003) MicroRNAs and small interfering RNAs can inhibit mRNA expression by similar mechanisms. *Proc. Natl Acad Sci. USA*, **100**, 9779–9784.
9. Yekta,S., Shih,I.H. and Bartel,D.P. (2004) MicroRNA-directed cleavage of HOXB8 mRNA. *Science*, **304**, 594–596.
10. Bagga,S., Bracht,J., Hunter,S., Massirer,K., Holtz,J., Eachus,R. and Pasquinelli,A.E. (2005) Regulation by let-7 and lin-4 miRNAs results in target mRNA degradation. *Cell*, **122**, 553–563.
11. Doench,J.G., Petersen,C.P. and Sharp,P.A. (2003) siRNAs can function as miRNAs. *Genes Dev*, **17**, 438–442.
12. Petersen,C.P., Bordeleau,M.E., Pelletier,J. and Sharp,P.A. (2006) Short RNAs repress translation after initiation in mammalian cells. *Mol. Cell*, **21**, 533–542.
13. Olsen,P.H. and Ambros,V. (1999) The lin-4 regulatory RNA controls developmental timing in *Caenorhabditis elegans* by blocking LIN-14 protein synthesis after the initiation of translation. *Dev. Biol.*, **216**, 671–680.
14. Jing,Q., Huang,S., Guth,S., Zarubin,T., Motoyama,A., Chen,J., Di Padova,F., Lin,S.C., Gram,H. and Han,J. (2005) Involvement of microRNA in AU-rich element-mediated mRNA instability. *Cell*, **120**, 623–634.
15. Cullen,B.R. (2004) Transcription and processing of human microRNA precursors. *Mol. Cell*, **16**, 861–865.
16. Lee,Y., Jeon,K., Lee,J.T., Kim,S. and Kim,V.N. (2002) MicroRNA maturation: stepwise processing and subcellular localization. *Embo J.*, **21**, 4663–4670.
17. Cai,X., Hagedorn,C.H. and Cullen,B.R. (2004) Human microRNAs are processed from capped, polyadenylated transcripts that can also function as mRNAs. *RNA*, **10**, 1957–1966.
18. Lee,Y., Kim,M., Han,J., Yeom,K.H., Lee,S., Baek,S.H. and Kim,V.N. (2004) MicroRNA genes are transcribed by RNA polymerase II. *Embo J.*, **23**, 4051–4060.
19. Lee,Y., Ahn,C., Han,J., Choi,H., Kim,J., Yim,J., Lee,J., Provost,P., Radmark,O., Kim,S. *et al.* (2003) The nuclear RNase III Drosha initiates microRNA processing. *Nature*, **425**, 415–419.
20. Suh,M.R., Lee,Y., Kim,J.Y., Kim,S.K., Moon,S.H., Lee,J.Y., Cha,K.Y., Chung,H.M., Yoon,H.S., Moon,S.Y. *et al.* (2004) Human embryonic stem cells express a unique set of microRNAs. *Dev Biol.*, **270**, 488–498.
21. He,L., Thomson,J.M., Hemann,M.T., Hernando-Monge,E., Mu,D., Goodson,S., Powers,S., Cordon-Cardo,C., Lowe,S.W., Hannon,G.J. *et al.* (2005) A microRNA polycistron as a potential human oncogene. *Nature*, **435**, 828–833.
22. Baskerville,S. and Bartel,D.P. (2005) Microarray profiling of microRNAs reveals frequent coexpression with neighboring miRNAs and host genes. *RNA*, **11**, 241–247.
23. McManus,M.T. and Sharp,P.A. (2002) Gene silencing in mammals by small interfering RNAs. *Nat. Rev. Genet.*, **3**, 737–747.
24. Yu,J.Y., Wang,T.W., Vojtek,A.B., Parent,J.M. and Turner,D.L. (2005) Use of short hairpin RNA expression vectors to study mammalian neural development. *Methods Enzymol.*, **392**, 186–199.
25. Yu,J.Y., Taylor,J., DeRuiter,S.L., Vojtek,A.B. and Turner,D.L. (2003) Simultaneous inhibition of GSK3alpha and GSK3beta using hairpin siRNA expression vectors. *Mol. Ther.*, **7**, 228–236.
26. Jazag,A., Kanai,F., Ijichi,H., Tateishi,K., Ikenoue,T., Tanaka,Y., Ohta,M., Imamura,J., Guleng,B., Asaoka,Y. *et al.* (2005) Single small-interfering RNA expression vector for silencing multiple

transforming growth factor-beta pathway components. *Nucleic Acids Res*., **33**, e131.
27. Zeng,Y., Wagner,E.J. and Cullen,B.R. (2002) Both natural and designed micro RNAs can inhibit the expression of cognate mRNAs when expressed in human cells. *Mol. Cell*., **9**, 1327–1333.
28. Zeng,Y., Cai,X. and Cullen,B.R. (2005) Use of RNA polymerase II to transcribe artificial microRNAs. *Methods Enzymol*., **392**, 371–380.
29. Zhou,H., Xia,X.G. and Xu,Z. (2005) An RNA polymerase II construct synthesizes short-hairpin RNA with a quantitative indicator and mediates highly efficient RNAi. *Nucleic Acids Res*., **33**, e62.
30. Boden,D., Pusch,O., Silbermann,R., Lee,F., Tucker,L. and Ramratnam,B. (2004) Enhanced gene silencing of HIV-1 specific siRNA using microRNA designed hairpins. *Nucleic Acids Res*., **32**, 1154–1158.
31. Silva,J.M., Li,M.Z., Chang,K., Ge,W., Golding,M.C., Rickles,R.J., Siolas,D., Hu,G., Paddison,P.J., Schlabach,M.R. *et al*. (2005) Second-generation shRNA libraries covering the mouse and human genomes. *Nature Genet*., **37**, 1281–1288.
32. Stegmeier,F., Hu,G., Rickles,R.J., Hannon,G.J. and Elledge,S.J. (2005) A lentiviral microRNA-based system for single-copy polymerase II-regulated RNA interference in mammalian cells. *Proc. Natl Acad. Sci. USA*, **102**, 13212–13217.
33. Xia,H., Mao,Q., Paulson,H.L. and Davidson,B.L. (2002) siRNA-mediated gene silencing *in vitro* and *in vivo*. *Nat. Biotechnol*, **20**, 1006–1010.
34. Rao,M.K., Pham,J., Imam,J.S., Maclean,J.A., Murali,D., Furuta,Y., Sinha-Hikim,A.P. and Wilkinson,M.F. (2006) Tissue-specific RNAi reveals that WT1 expression in nurse cells controls germ cell survival and spermatogenesis. *Genes Dev*., **20**, 147–152.
35. Tam,W. (2001) Identification and characterization of human BIC, a gene on chromosome 21 that encodes a noncoding RNA. *Gene*, **274**, 157–167.
36. Tam,W., Ben-Yehuda,D. and Hayward,W.S. (1997) bic, a novel gene activated by proviral insertions in avian leukosis virus-induced lymphomas, is likely to function through its noncoding RNA. *Mol. Cell Biol*., **17**, 1490–1502.
37. Tam,W. and Dahlberg,J.E. (2006) miR-155/BIC as an oncogenic microRNA. *Genes Chromosomes Cancer*, **45**, 211–212.
38. Lagos-Quintana,M., Rauhut,R., Yalcin,A., Meyer,J., Lendeckel,W. and Tuschl,T. (2002) Identification of Tissue-Specific MicroRNAs from Mouse. *Curr. Biol*., **12**, 735–739.
39. Tam,W., Hughes,S.H., Hayward,W.S. and Besmer,P. (2002) Avian bic, a gene isolated from a common retroviral site in avian leukosis virus-induced lymphomas that encodes a noncoding RNA, cooperates with c-myc in lymphomagenesis and erythroleukemogenesis. *J. Virol*., **76**, 4275–4286.
40. Farah,M.H., Olson,J.M., Sucic,H.B., Hume,R.I., Tapscott,S.J. and Turner,D.L. (2000) Generation of neurons by transient expression of neural bHLH proteins in mammalian cells. *Development*, **127**, 693–702.
41. Turner,D.L. and Weintraub,H. (1994) Expression of achaete-scute homolog 3 in *Xenopus* embryos converts ectodermal cells to a neural fate. *Genes Dev*., **8**, 1434–1447.
42. Rupp,R.A., Snider,L. and Weintraub,H. (1994) *Xenopus* embryos regulate the nuclear localization of XMyoD. *Genes Dev*., **8**, 1311–1323.
43. Matsuda,T. and Cepko,C.L. (2004) Electroporation and RNA interference in the rodent retina *in vivo* and *in vitro*. *Proc. Natl Acad. Sci. USA*, **101**, 16–22.
44. Lee,J.E., Hollenberg,S.M., Snider,L., Turner,D.L., Lipnick,N. and Weintraub,H. (1995) Conversion of Xenopus ectoderm into neurons by NeuroD, a basic helix–loop–helix protein. *Science*, **268**, 836–844.
45. Wang,X. and Seed,B. (2003) A PCR primer bank for quantitative gene expression analysis. *Nucleic Acids Res*., **31**, e154.
46. Zeng,Y., Yi,R. and Cullen,B.R. (2005) Recognition and cleavage of primary microRNA precursors by the nuclear processing enzyme Drosha. *Embo J*., **24**, 138–148.
47. Johansen,T.E., Scholler,M.S., Tolstoy,S. and Schwartz,T.W. (1990) Biosynthesis of peptide precursors and protease inhibitors using new constitutive and inducible eukaryotic expression vectors. *FEBS Lett*., **267**, 289–294.
48. Reynolds,A., Leake,D., Boese,Q., Scaringe,S., Marshall,W.S. and Khvorova,A. (2004) Rational siRNA design for RNA interference. *Nat. Biotechnol*., **22**, 326–330.
49. Elbashir,S.M., Lendeckel,W. and Tuschl,T. (2001) RNA interference is mediated by 21- and 22-nucleotide RNAs. *Genes Dev*., **15**, 188–200.
50. Llave,C., Xie,Z., Kasschau,K.D. and Carrington,J.C. (2002) Cleavage of Scarecrow-like mRNA targets directed by a class of *Arabidopsis* miRNA. *Science*, **297**, 2053–2056.
51. Yu,J.Y., DeRuiter,S.L. and Turner,D.L. (2002) RNA interference by expression of short-interfering RNAs and hairpin RNAs in mammalian cells. *Proc. Natl Acad. Sci. USA*, **99**, 6047–6052.
52. Dickins,R.A., Hemann,M.T., Zilfou,J.T., Simpson,D.R., Ibarra,I., Hannon,G.J. and Lowe,S.W. (2005) Probing tumor phenotypes using stable and regulated synthetic microRNA precursors. *Nature Genet*., **37**, 1289–1295.
53. Zeng,Y. and Cullen,B.R. (2003) Sequence requirements for micro RNA processing and function in human cells. *RNA*, **9**, 112–123.
54. Unwalla,H.J., Li,H.T., Bahner,I., Li,M.J., Kohn,D. and Rossi,J.J. (2006) Novel Pol II fusion promoter directs human immunodeficiency virus type 1-inducible coexpression of a short hairpin RNA and protein. *J. Virol*, **80**, 1863–1873.
55. Samakoglu,S., Lisowski,L., Budak-Alpdogan,T., Usachenko,Y., Acuto,S., Di Marzo,R., Maggio,A., Zhu,P., Tisdale,J.F., Riviere,I. *et al*. (2006) A genetic strategy to treat sickle cell anemia by coregulating globin transgene expression and RNA interference. *Nat. Biotechnol*, **24**, 89–94.
56. Xia,X.G., Zhou,H., Samper,E., Melov,S. and Xu,Z. (2006) Pol II-expressed shRNA knocks down Sod2 gene expression and causes phenotypes of the gene knockout in mice. *PLoS Genet*, **2**, e10.
57. Huang,Y. and Carmichael,G.C. (1996) Role of polyadenylation in nucleocytoplasmic transport of mRNA. *Mol. Cell. Biol*., **16**, 1534–1542.
58. Eis,P.S., Tam,W., Sun,L., Chadburn,A., Li,Z., Gomez,M.F., Lund,E. and Dahlberg,J.E. (2005) Accumulation of miR-155 and BIC RNA in human B cell lymphomas. *Proc. Natl Acad. Sci. USA*, **102**, 3627–3632.
59. Zeng,Y. and Cullen,B.R. (2005) Efficient processing of primary microRNA hairpins by Drosha requires flanking nonstructured RNA sequences. *J. Biol. Chem*., **280**, 27595–27603.
60. Zeng,Y. and Cullen,B.R. (2004) Structural requirements for pre-microRNA binding and nuclear export by Exportin 5. *Nucleic Acids Res*., **32**, 4776–4785.
61. Vermeulen,A., Behlen,L., Reynolds,A., Wolfson,A., Marshall,W.S., Karpilow,J. and Khvorova,A. (2005) The contributions of dsRNA structure to Dicer specificity and efficiency. *RNA*, **11**, 674–682.
62. Zuker,M. (2003) Mfold web server for nucleic acid folding and hybridization prediction. *Nucleic Acids Res*., **31**, 3406–3415.